Unified Flicker Noise Model

Colin McAndrew
Freescale Semiconductor
Tempe, AZ

Abstract

The book (*Operation and Modeling of the MOS Transistor, 3rd Edition,* by Yannis Tsividis and Colin McAndrew, Oxford University Press, 2011) discusses noise models in Chaps. 7 and 8. The unified flicker noise model, which is widely used in compact MOS transistor models, was not detailed in the book because of its complexity (see p. 453, Chap. 7); details of this model and its derivation are provided here.

Copyright © 2011 by Oxford University Press

Unified Flicker Noise Model

As shown in Fig. 7.31 in the book, at low frequencies flicker noise is dominant. This noise is also called "$1/f$" noise because the power spectral density is nearly proportional to the inverse of the frequency. Note that this does not imply that flicker noise only affects circuits at low frequencies; if two signals of frequencies f_1 and f_2 are passed through a nonlinear circuit then the output of the circuit contains not just components at these two frequencies, but also has components at integer sums and differences $nf_1 \pm mf_2$ of the frequencies. These frequency translations can "up-convert" low frequency noise into the frequency range that is of importance for a particular circuit; hence flicker noise can be important for RF circuits, such as oscillators [1].

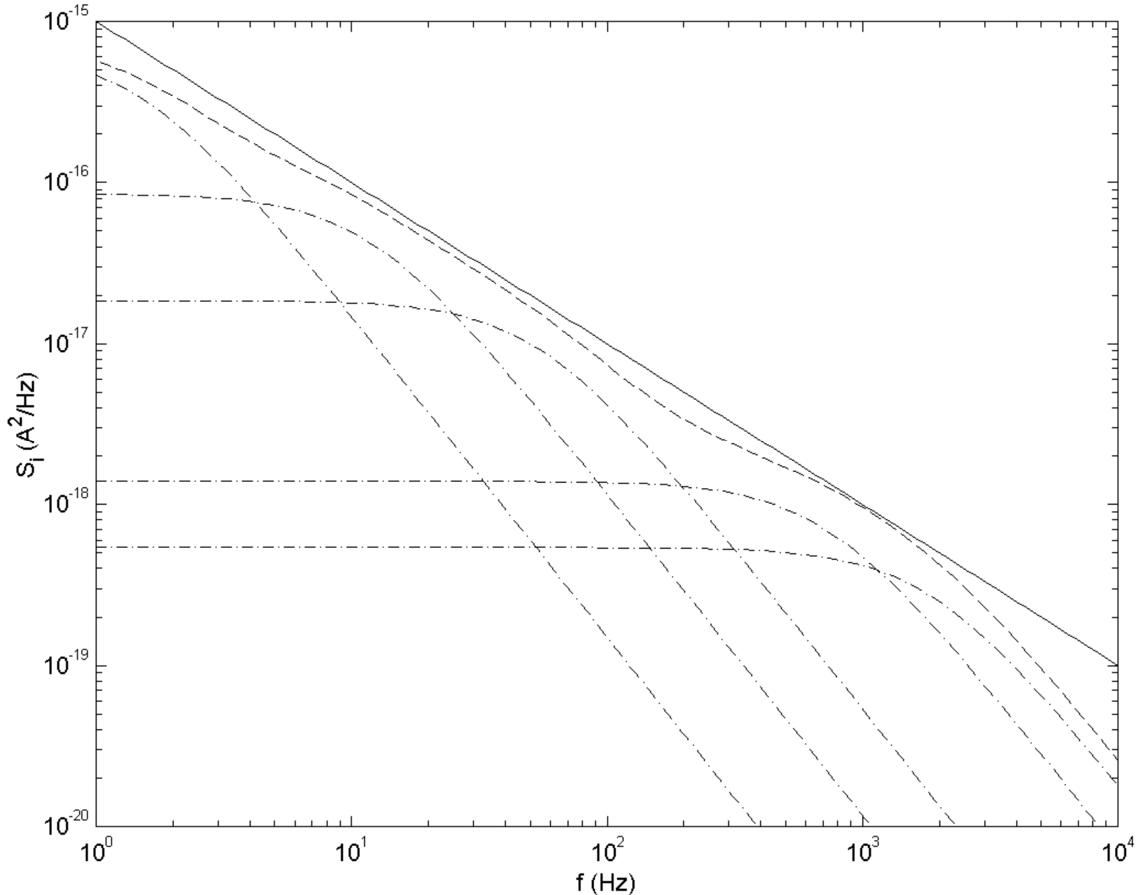

Fig. 1 Drain current noise spectral power density versus frequency. Solid line is ideal $1/f$ characteristic. Dash-dot lines are Lorentzian spectra from 5 traps with random time constants. Dashed line is the sum of the 5 individual trap spectra; even with only 5 traps it well approximates $1/f$ behavior (Fig. 7.37 in the book).

There are two main theories that have been proposed to explain flicker noise. The first is attributed to random fluctuations in the number of carriers in the channel [2][3], based on the statistical time dependence of the capture and release of carriers by traps in the gate dielectric (spatially localized levels in the energy band structure caused by imperfections in the lattice structure that are available for carriers to occupy). The second is attributed to mobility fluctuations due to carrier interactions with lattice vibrations (i.e. with phonons) [4][5]. By noting that the carrier number fluctuations can be correlated to mobility through Coulomb scattering, a so-called "unified" $1/f$ noise model has been developed [6][7][8][9]. Note that this approach does not merge the separate random dopant fluctuation and mobility fluctuation theories; it *adds* a correlated mobility fluctuation term to a random dopant fluctuation theory. Although it has been argued that the correlated mobility fluctuations are negligible for *p*MOS transistors [10], detailed experimental results show similarities in the noise spectra of

Copyright © 2011 by Oxford University Press

*p*MOS and *n*MOS transistors, where for small gate areas the effects of individual traps become evident [11]. Further support that traps affect 1/*f* noise comes from experiments which show that applying a large voltage on the gate induces an increase in the number of traps, and this correlates to increased flicker noise [6]. The unified flicker noise model has therefore become widely, although not universally, accepted.

The power spectral density of the fluctuation in the number of carriers N from recombination and generation processes, if the lifetime of the carriers is τ_t and there is no restriction on the rates at which these processes occur, is given by [11]

$$S_N(f) = 4\overline{\Delta N}^2 \frac{t_t}{1+\omega^2\tau_t^2} \tag{1}$$

where $\overline{\Delta N}^2$ is the variance of the number of carriers and $\omega = 2\pi f$ is angular frequency. This type of spectrum is called Lorentzian. Notice that it does not have a 1/*f* characteristic; rather, it is constant at low frequencies and decreases as $1/f^2$ at high frequencies. However, as Fig. 1 shows, the sum of a number of Lorentzian spectra, from traps with different values for τ_t closely approximates a 1/*f* characteristic. This is observed for both *n*MOS [13][14] and *p*MOS [11] transistors. Fig. 2 shows measured noise spectra of identical *n*MOS devices measured at 5 different sites on a wafer. An approximate Lorentzian characteristic is discernable for some of the devices, and the variation between devices is significant. This is consistent with the number of traps, and their characteristic time constants, varying statistically between devices. For larger area devices the variation between devices decreases and the overall flicker noise more closely approximates a 1/*f* characteristic [11][14][15], as would be expected from averaging of a larger number of traps.

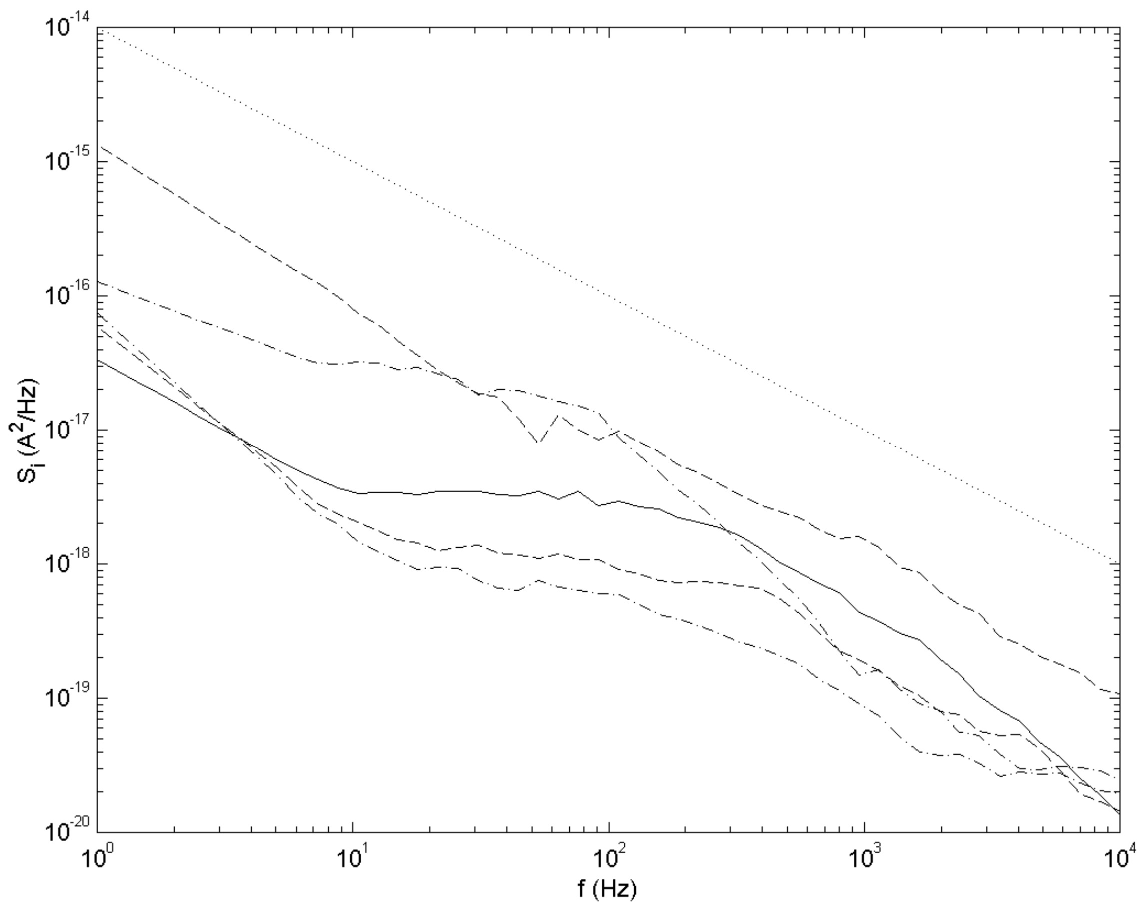

Fig. 2 Measured noise characteristics of identical *W*/*L*=0.7μm/0.28μm *n*MOS devices from 5 different sites on a wafer, $V_{GS} = 1.1$ V and $V_{DS} = 1.0$ V. Dotted line is 1/*f* reference slope (Fig. 7.38 in the book).

Copyright © 2011 by Oxford University Press

For electrons becoming captured or released from traps in the dielectric above the silicon surface, the probability of a transition between these two states depends on the product of the relative occupancy levels of the energies of both the initial and final states; for electron levels in the silicon this is determined by Fermi-Dirac statistics. Detailed analysis shows that, predominantly, the energies of the electrons involved must be near the electron quasi-Fermi level, E_{fn}, or else the number of occupied or available states in the silicon is small. Assuming that the probability of an electron tunneling to an available trap site in the gate dielectric decreases exponentially with the distance of the trap from the silicon-dielectric interface, so the time constant τ_t associated with a trap increases exponentially with this distance, integration over the available energy states and the extend of the dielectric gives [16][9]

$$(2) \qquad S_N(f) \approx N_{it}^{'}(E_{fn}) \frac{kT}{10^8 f^{E_F}}$$

where the 10^8 factor (in units of cm^{-1}), which is approximate, comes from analysis of the tunneling probability, $N_{it}^{'}(E_{fn})$ is the occupied interface trap density, in cm^{-2}, at the electron quasi-Fermi level, and E_F is a fitting parameter. Experimental data show that the exponent of frequency E_F can deviate from 1, and vary from roughly 0.7 to 1.2. This has been quantitatively explained by the trap distribution in the gate dielectric not being uniform, but varying with distance from the interface [16]; hence the introduction of E_F.

To determine the effect of the statistical variation in the density of trapped electrons on the drain current, we need first to relate it to the variation in the inversion charge density, and in turn relate that to the variation in drain current. Although most of our analysis will be based on strong inversion approximations, one feature of the unified model is that it reasonably approximates flicker noise in weak and moderate inversion; it is inclusion of the first of these steps, the balance between inversion charge and trapped charge densities, which enables this.

The interface traps are taken to be distributed randomly across the area of the transistor, with a density $N_{it}^{'}$ which is a function of position within the channel (the available trap sites within the gate dielectric are uniformly distributed, however the occupied trap density depends on the inversion charge density, which is a function of position). The interface charge $Q_0^{'}$, as discussed in Sec. 2.2, needs to be separated into a fixed component $Q_{0F}^{'}$, that does not change over a time scale associated with flicker noise variations, and a component $Q_{it}^{'} = -qN_{it}^{'}$ associated with the time-varying trapped charge. The charge balance relation (2.3.4) is then

$$(3) \qquad Q_G^{'} + (Q_{0F}^{'} + Q_{it}^{'}) + Q_I^{'} + Q_B^{'} = 0 .$$

If the fluctuation in the inversion carrier density, $N_I^{'} = -Q_I^{'}/q$, caused by the fluctuation in the trapped electron density is denoted R

$$(4) \qquad R = \frac{\partial N_I^{'}}{\partial N_{it}^{'}} = -\frac{1}{q}\frac{\partial Q_I^{'}}{\partial N_{it}^{'}}$$

then a change $\Delta N_{it}^{'}$ in the occupied interface trap density because some carriers are captured or released from traps will lead to a change in the inversion charge density of [17][18][9]

$$(5) \qquad \Delta Q_I^{'} = -qR\,\Delta N_{it}^{'} .$$

In strong inversion there is essentially a 1-to-1 exchange of electrons between the inversion charge and the trapped charge, so R is close to -1 (for every electron captured by a trap one electron is lost from the inverted channel); in weak inversion its magnitude becomes smaller than 1 as a change in the trapped charge balances changes in other charge components as well [19]. Differentiating with respect to ψ_s allows the change in $Q_{it}^{'}$ to be related to changes in the other charges, and using this gives

$$(6) \qquad R = -\frac{1}{q}\frac{\partial Q_I^{'}/\partial\psi_s}{\partial N_{it}^{'}/\partial\psi_s} \approx -\left(\frac{\partial Q_I^{'}/\partial\psi_s}{\partial Q_I^{'}/\partial\psi_s + \partial Q_G^{'}/\partial\psi_s + \partial Q_B^{'}/\partial\psi_s}\right).$$

Copyright © 2011 by Oxford University Press

In weak inversion $\partial Q_I^{'} / \partial \psi_s$ is approximately $Q_I^{'} / \phi_t$ (see (2.6.28)) and in strong inversion reduces to $0.5 Q_I^{'} / \phi_t$ (see (2.6.8), where in strong inversion the exponential term dominates). As noted $R \approx -1$ in strong inversion, and $\partial Q_I^{'} / \partial \psi_s$ is much greater than any of the other terms in (6), see Fig. 2.23, so imprecision in that term in strong inversion is of little consequence; we will therefore use the weak inversion approximation for $\partial Q_I^{'} / \partial \psi_s$. Recognizing that $\partial Q_G^{'} / \partial \psi_s = -C_{ox}^{'}$ and $\partial Q_B^{'} / \partial \psi_s = -C_b^{'}$ of (2.7.14), which is the depletion layer incremental capacitance per unit area, we can therefore write (6) as

$$(7) \qquad R = -\left(\frac{(-Q_I^{'})}{(-Q_I^{'}) + \phi_t (C_{ox}^{'} + C_b^{'})} \right).$$

In some treatments [9][18] an additional component is included

$$(8) \qquad R = -\left(\frac{(-Q_I^{'})}{(-Q_I^{'}) + \phi_t (C_{ox}^{'} + C_b^{'} + C_{IT})} \right)$$

where $C_{IT} = C_{it}^{'}$ is associated with the interface traps and is given by (2.7.26); as $C_{it}^{'}$ is not usually determined as part of a MOS transistor characterization procedure C_{IT} is introduced as a fitting parameter, to be adjusted to best fit measured flicker noise data.

Again we stress that although our analysis is generally based on strong inversion operation, the characterization of R is based on weak inversion operation. However, in strong inversion the $Q_I^{'}$ term in (7) dominates and gives the correct result $R \approx -1$ [17][19]. The result (7) is therefore valid in strong inversion, and as the accuracy of in the unified flicker noise model in weak (and moderate) inversion depends on the characterization of R this approach is reasonable.

Now we investigate how fluctuations in the inversion charge density cause variations in the drain current. Consider the drift component of drain current, which is the dominant component in strong inversion

$$(9) \qquad I_{DS}(x) = \mu W (-Q_I^{'}(x)) \frac{\partial \psi_s}{\partial x}.$$

A change $\Delta N_{it}^{'}$ in the occupied trap density will affect this current in two ways. First, from the previous discussion there will be a change $\Delta Q_I^{'}$ in the inversion charge density. In addition, because of Coulomb scattering (Sec. 4.11) the mobility will also change. Although the surface potential should change as well, in strong inversion ψ_s is almost pinned at $\phi_0 + V_{CB}$ so we will ignore the small variations induced in ψ_s. Therefore the change in drain current Δi associated with the change in the number of carriers in traps is, using (4),

$$(10) \qquad \Delta i = W \frac{\partial \psi_s}{\partial x} \left(\mu \frac{\partial (-Q_I^{'})}{\partial N_{it}^{'}} \pm (-Q_I^{'}) \frac{\partial \mu}{\partial N_{it}^{'}} \right) \Delta N_{it}^{'} = I_{DS} \left(q \frac{R}{(-Q_I^{'})} \pm \frac{1}{\mu} \frac{\partial \mu}{\partial N_{it}^{'}} \right) \Delta N_{it}^{'}$$

where the + or - sign depends on whether a trap is neutral or charged when filled, which will increase or decrease surface mobility, respectively. (Using a drain current formulation in terms of the electron quasi-Fermi level, see (F.9), this result is also valid in weak and moderate inversion, assuming the quasi-Fermi level is not perturbed by the change in charge densities). The inclusion of the mobility dependence on the occupied trap density is how mobility fluctuations are incorporated in the unified flicker noise model. To determine the power spectral density for the drain current we need to integrate the fluctuations in Δi^2, from (10), along the channel, so using (2) and recognizing that the variation in total occupied traps, as opposed to the trap density, also needs to be averaged over the channel, we have

$$(11) \qquad S_{if}(f) = \frac{kTq^2 I_{DS}^2}{10^8 W L^2 f^{E_F}} \int_0^L N_{it}^{'}(E_{fn}) \left(1 \pm \frac{1}{\mu} \frac{\partial \mu}{\partial N_{it}^{'}} \frac{(-Q_I^{'})}{qR} \right)^2 \left(\frac{R}{(-Q_I^{'})} \right)^2 dx.$$

Copyright © 2011 by Oxford University Press

Some treatments then correlate the mobility change to the trap density change [7], however the most widely used unified flicker noise model instead assumes that [9]

$$(12)\qquad N'_{it}(E_{fn})\left(1 \pm \frac{1}{\mu}\frac{\partial\mu}{\partial N'_{it}}\frac{(-Q'_I)}{qR}\right)^2 = N_{OIA} + N_{OIB}(-Q'_I) + N_{OIC}(-Q'_I)^2$$

where N_{OIA}, N_{OIB}, and N_{OIC} are empirical parameters. Notice that this has removed the explicit physical correlation between variation in the mobility and variation in the trapped charge density; there is now an implicit dependence through the values of the empirical parameters as determined from experimental data. Using (12) in (11) we have

$$(13)\qquad S_{if}(f) = \frac{kTq^2 I_{DS}^2}{10^8 WL^2 f^{E_F}} \int_0^L \left(N_{OIA} + N_{OIB}(-Q'_I) + N_{OIC}(-Q'_I)^2\right)\frac{R^2}{(-Q'_I)^2}\,dx\,.$$

Now using (4.4.15) in (9) gives

$$(14)\qquad I_{DS} = \mu W \frac{(-Q'_I)}{\alpha C'_{ox}}\frac{\partial Q'_I}{\partial x}$$

where α is given by (4.4.2) and for now we will not specify an expansion point ψ_{se} around which ψ_s is linearized as it is different for different model forms. This allows the integration variable in (13) to be changed from x to Q'_I, which gives, using (7),

$$(15)\qquad S_{if}(f) = \frac{\mu kTq^2 I_{DS}}{10^8 \alpha L^2 C'_{ox} f^{E_F}} \int_{-Q'_{IL}}^{-Q'_{I0}} \left(N_{OIA} + N_{OIB}(-Q'_I) + N_{OIC}(-Q'_I)^2\right)\frac{(-Q'_I)}{\left((-Q'_I) + \phi_t(C'_{ox} + C'_b + C_{IT})\right)^2}\,d(-Q'_I)$$

where Q'_{I0} and Q'_{IL} are the inversion charge density at the source and drain end of the channel, respectively, and they are computed from either the surface potential, for a charge sheet model, or the terminal biases and the threshold voltage, for a threshold voltage based model.

For generality we need to consider operation in saturation as well as nonsaturation. For operation in saturation we will consider, as in Sec. 5.3, there to be a region of length l_p at the drain end of the transistor where the channel is in pinchoff. We will further assume that the inversion charge density in this region is uniform and of value Q'_{IL}; as a device is operated further into saturation the pinchoff point will move further away from the drain and into the channel, so l_p will increase, but the inversion charge density at both the left and right ends of the pinchoff reason remain at Q'_{IL}, which is calculated at V'_{DS}. For the portion of the channel that is not in pinchoff we can use (15); for the portion of the channel in pinchoff we can use (13), but with a lower bound for the integration of $L - l_p$.

The three components of the integral in (15) lead to a fairly complex expression for the spectral density, however several of the terms are small; keeping only the dominant terms gives, in saturation,

$$(16)\qquad \begin{aligned} S_{if}(f) = {} & \frac{\mu kTq^2 I_{DS}}{10^8 \alpha L^2 C'_{ox} f^{E_F}} \left(N_{OIA} \ln\left(\frac{(-Q'_{I0}) + \phi_t(C'_{ox} + C'_b + C_{IT})}{(-Q'_{IL}) + \phi_t(C'_{ox} + C'_b + C_{IT})}\right) + N_{OIB}\left((-Q'_{I0}) - (-Q'_{IL})\right) \right. \\ & \left. + 0.5 N_{OIC}\left((-Q'_{I0})^2 - (-Q'_{IL})^2\right)\right) + l_p \frac{kTq^2 I_{DS}^2}{10^8 WL^2 f^{E_F}} \frac{N_{OIA} + N_{OIB}(-Q'_{IL}) + N_{OIC}(-Q'_{IL})^2}{\left((-Q'_{IL}) + \phi_t(C'_{ox} + C'_b + C_{IT})\right)^2}\,. \end{aligned}$$

For source-referenced models, α and C'_b are evaluated based on V_{SB}. For the symmetric linearization charge sheet model they are evaluated at the mid-point surface potential ψ_{sm}. The flicker noise varies by orders of magnitude from weak inversion to strong inversion, and these quantities change only weakly with bias, so it is not critical exactly how they are

Copyright © 2011 by Oxford University Press

calculated; any slight imprecision in these terms can be offset by adjusting values for the N_{OIA}, N_{OIB}, and N_{OIC} parameters.

In nonsaturation operation, $l_p = 0$, the last term in (16) becomes zero, and Q'_{IL} is calculated from V_{DS}, and not from V'_{DS} as it is for saturation operation.

The model (16) appears somewhat complex, and clearly there are several approximations made in deriving it. However, this unified flicker noise model, or variations of it, are widely used and have proven to fit experimental data reasonably well. In particular, because of the charge balancing factor *R* it models the significant variation in flicker noise from weak inversion through strong inversion, see Fig. 3.

Notice, in comparison with (4.4.17*b*) and (4.4.17*a*), that the first terms in N_{OIB} and N_{OIC} in (16) are related to the diffusion and drift components of drain current, respectively. In this way these parameters can be seen to, conveniently, provide independent fitting of data in weak and strong inversion, respectively. In fact if the term in N_{OIC} is the dominant component, then using (4.4.17*a*) gives

$$(17) \qquad S_{if}(f) = \frac{N_{OIC} kTq^2 I_{DS}^2}{10^8 LWf^{E_F}} .$$

This is a form of flicker noise model that was used in early SPICE MOS transistor models [20].

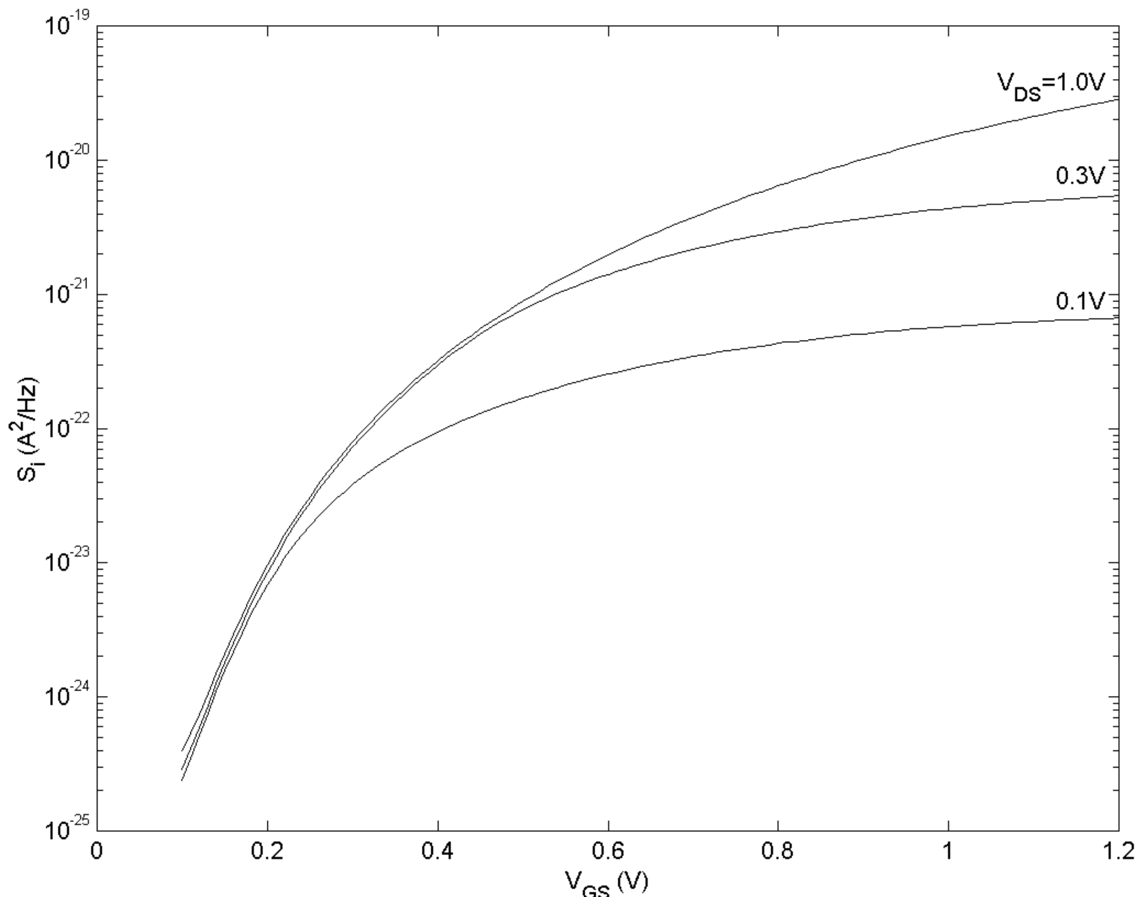

Fig. 3 Drain current flicker noise power spectral density as a function of V_{GS}, *f*=100 Hz, *W*/*L*=10µm/10µm.

Copyright © 2011 by Oxford University Press

References

[1] T. H. Lee and A. Hajimiri, "Oscillator phase noise: a tutorial," *IEEE Journal of Solid-State Circuits*, vol. 35, no. 3, pp. 326-336, March 2000.

[2] A. L. McWorther, "1/f noise and related surface effects in germanium," Massachusetts Institute of Technology Lincoln Laboratory Report 80, May 1955.

[3] A. L McWorther, "1/f noise and germanium surface properties," in *Semiconductor Surface Physics*, pp. 207-228, Philadelphia: University of Pennsylvania Press, 1957.

[4] F. N. Hooge, "1/f noise," *Physica*, vol. 83B, pp. 14-23, 1976.

[5] F. N. Hooge and L. K. Vandamme, "Lattice scattering causes 1/f noise," *Physics Letters*, vol. 66A, pp. 315-316, 1978.

[6] H. Mikoshiba, "1/f noise in n-channel silicon-gate MOS transistors," *IEEE Transactions on Electron Devices*, vol. ED-29, no. 6, pp. 965-970, June 1982.

[7] R. Jayaram and C. Sodini, "A 1/f noise technique to extract the oxide trap density near the conduction band edge of silicon," *IEEE Transactions on Electron Devices*, vol. 36, no. 9, pp. 1773-1782, September 1989.

[8] K. K. Hung, P. K. Ko, C. Hu, and Y. C. Cheng, "A unified model for the flicker noise in metal-oxide-semiconductor field-effect transistors," *IEEE Transactions on Electron Devices*, vol. 37, no. 3, pp. 654-665, March 1990.

[9] K. K. Hung, P. K. Ko, C. Hu, and Y. C. Cheng, "A physics-based MOSFET noise model for circuit simulators," *IEEE Transactions on Electron Devices*, vol. 37, no. 5, pp. 1323-1333, May 1990.

[10] E. P. Vandamme and L. K. J. Vandamme, "Critical discussion on unified 1/f noise models for MOSFETs," *IEEE Transactions on Electron Devices*, vol. 47, no. 11, pp. 2146-2152, November 2000.

[11] A. J. Scholten, L. F. Tiemeijer, R. van Langevelde, R. J. Havens, A. T. A. Zegers-van Duijnhoven, and V. C. Venezia, "Noise modeling for RF CMOS circuit simulation," *IEEE Transactions on Electron Devices*, vol. 50, no. 3, pp. 618-632, March 2003.

[12] A. van der Ziel, *Noise in Sold State Devices and Circuits*, Wiley Interscience, New York, 1986.

[13] R. Brederlow, W. Weber, D. Schmitt-Landsiedel, and R. Thewes, "Fluctuations af the low frequency noise of MOS transistors and their modeling in analog and RF-circuits," *Technical Digest of the International Electron Devices Meeting*, pp. 159-162, December 1999.

[14] G. I. Wirth, J. Koh, R. da Silva, R. Thewes, and R. Brederlow, "Modeling of statistical low-frequency noise of deep-submicrometer MOSFETs," *IEEE Transactions on Electron Devices*, vol. 52, no. 7, pp. 1576-1588, July 2005.

[15] M. Erturk, T. Xia, R. Anna, K. M. Newton, and E. Adler, "Statistical BSIM model sofr MOSFET 1/f noise," *Electronics Letters*, vol. 41, no. 22, pp. 1208-1209, October 2005.

[16] S. Christensson, I. Lundstrom, and C. Svensson, "Low frequency noise in MOS transistors – I theory," *Solid-State Electronics*, vol. 11, no. 9, pp. 797-812, September 1968.

[17] R. P. Jindal and A. van der Ziel, "Carrier fluctuation noise in a MOSFET channel due to traps in the oxide," *Solid-State Electronics*, vol. 21, no. 6, pp. 901-903, June 1978.

[18] G. Reimbold, "Modified 1/f trapping noise theory and experiments in MOS transistors biased from weak to strong inversion – influence of interface states," *IEEE Transactions on Electron Devices*, vol. ED-31, no. 9, pp. 1190-1198, September 1984.

Copyright © 2011 by Oxford University Press

[19] L. D. Yau and C.-T. Sah, “Theory and experiments of low-frequency generation-recombination noise in MOS transistors,” *IEEE Transactions on Electron Devices*, vol. ED-16, no. 2, pp. 170-177, February 1969.

[20] G. Massobrio and P. Antognetti, *Semiconductor Device Modeling with SPICE*, McGraw-Hill, New York,1993.

Copyright © 2011 by Oxford University Press